Local regulation of the threshold for calcium sparks in rat ventricular myocytes: role of sodium–calcium exchange

Joshua I. Goldhaber, Scott T. Lamp, Donald O. Walter, Alan Garfinkel, Gary H. Fukumoto and James N. Weiss

The Cardiovascular Research Laboratories, Departments of Medicine (Cardiology), Physiology, and Physiological Sciences, UCLA School of Medicine, Los Angeles, CA 90095-1679, USA

1. To determine whether Na^+–Ca^{2+} exchange modulates Ca^{2+} sparks, we studied enzymatically isolated patch clamped rat ventricular myocytes loaded with the Ca^{2+}-sensitive indicator fluo-3, using confocal microscopy at 20–22 °C. Two-dimensional images of Ca^{2+} sparks were recorded at 240 Hz using a laser scanning confocal microscope, allowing observation of a large area of the cell ($820~\mu m^2$) at one time.

2. At a holding potential of -75 mV, spontaneous sparks were infrequent. Removal of extracellular Na^+ for 520 ms, which in the absence of pipette Na^+ should block Na^+–Ca^{2+} exchange bidirectionally, was associated with a fourfold increase in spark frequency, without a significant change in cytoplasmic $[Ca^{2+}]$, sarcoplasmic reticulum (SR) Ca^{2+} content, or spark intensity, size or time course.

3. These findings are consistent with a model of excitation–contraction coupling in which Na^+–Ca^{2+} exchange locally regulates the resting Ca^{2+} concentration in the diadic cleft (T-tubule–SR junction), thereby modulating the threshold for triggering Ca^{2+} sparks.

In cardiac cells, it is commonly accepted that contraction is initiated when a relatively small amount of Ca^{2+} entering through voltage-dependent L-type Ca^{2+} channels triggers a much larger release of Ca^{2+} from the sarcoplasmic reticulum (SR). It has also been proposed that Na^+–Ca^{2+} exchange working in 'reverse' (Ca^{2+}-influx) mode may serve as a second source of trigger Ca^{2+} (LeBlanc & Hume, 1990; Levi *et al.* 1994; Litwin *et al.* 1998); however, this latter hypothesis is controversial (Sham *et al.* 1992, 1995; Adachi-Akahane *et al.* 1996; Sipido *et al.* 1997).

The development of laser scanning confocal fluorescence microscopy has led to the identification of spontaneous local Ca^{2+} transients in ventricular myocytes. These local Ca^{2+} transients, termed Ca^{2+} sparks, are thought to reflect the fundamental events of excitation–contraction (E–C) coupling in cardiac cells (Cheng *et al.* 1993; López-López *et al.* 1994). The study of Ca^{2+} spark behaviour has furthered our understanding of the local regulation of E–C coupling. A spark event occurs when Ca^{2+} stored in the SR is released by one or more ryanodine receptors (RyRs) into a restricted space, the diadic cleft. At the resting potential, only a few spark events are identified, presumably triggered by the infrequent and stochastic openings of sarcolemmal L-type Ca^{2+} channels as well as the less frequent stochastic openings of RyRs. The whole-cell Ca^{2+} transient elicited by a strong depolarization is thought to represent the recruitment and summation of large numbers of Ca^{2+} sparks in response to an increased number of open L-type Ca^{2+} channels (López-López *et al.* 1995; Cleemann *et al.* 1998).

The relationship between the magnitude of the Ca^{2+} current (I_{Ca}) and the extent of Ca^{2+} released by the SR is known as the gain function (Wier *et al.* 1994). The role of Na^+–Ca^{2+} exchange as an activator of Ca^{2+} sparks and a regulator of gain has been uncertain. López-López *et al.* (1995), for example, have shown that Ca^{2+} entry via Na^+–Ca^{2+} exchange, elicited by depolarizing to very high membrane potentials, does not trigger sparks. However, they did not examine how Na^+–Ca^{2+} exchange might influence spark frequency, a reflection of gain.

Since the open probability of the RyR has a sigmoidal dependence on $[Ca^{2+}]$ (Györke & Fill, 1993; Copello *et al.* 1997), it follows that any process that increases the local Ca^{2+} concentration near the cytoplasmic domain of a RyR should increase its open probability. This translates to an increase in gain since less additional Ca^{2+} is needed to further increase the open probability of the local RyR(s) to a regenerative threshold. The Na^+–Ca^{2+} exchanger, concentrated in the sarcolemmal membrane of the transverse tubules (Frank *et al.* 1992), could play an important role in modulating gain by setting the resting Ca^{2+} level in the diadic cleft. The exchanger could thereby regulate how much incremental Ca^{2+} entry into the cleft, via Ca^{2+} channel or RyR opening, is required to reach the

threshold for local regenerative Ca^{2+} release from RyRs in the diad (Litwin et al. 1998).

To determine whether Na^+–Ca^{2+} exchange can influence Ca^{2+} release at the microdomain level, we examined the consequences of modulating Na^+–Ca^{2+} exchange on Ca^{2+} spark characteristics in isolated rat ventricular myocytes, using the patch clamp technique in conjunction with 2-D laser scanning confocal microscopy. We find that Na^+–Ca^{2+} exchange can significantly influence Ca^{2+} spark frequency, without altering the spatial or kinetic characteristics of individual spark events.

METHODS

Patch clamp

Adult Sprague-Dawley rats (200–300 g) were killed with an overdose of sodium pentobarbitone in accordance with the guidelines of the UCLA Office for Protection of Research Subjects. Their hearts were removed and single ventricular myocytes were isolated using collagenase (2 mg ml^{-1}, Type II collagenase; Gibco BRL, Life Technologies, Gaithersburg, MD, USA) and protease (0·166 mg ml^{-1}, Type XIV protease; Sigma) digestion according to the method of Mitra & Morad (1985). The cells were stored in a modified Na^+-Tyrode solution, containing (mM): 136 NaCl, 5·4 KCl, 10 Hepes, 1 $MgCl_2$, 1·8 $CaCl_2$, 10 glucose, pH 7·4 with NaOH (temperature 20–22 °C). We selected for study only Ca^{2+}-tolerant cells that lacked spontaneous contractions. Patch electrodes were pulled from borosilicate glass (World Precision Instruments, Sarasota, FL, USA, TW150F-3) on a Sutter P-87 horizontal puller (Sutter Instruments, Novato, CA, USA). The electrodes had a tip diameter of 2–3 μm and a resistance of 2–4 MΩ after gentle fire-polishing and when filled with an internal solution containing (mM): 110 CsCl, 20 TEA-Cl, 20 Hepes, 5 MgATP (adenosine 5′-triphosphate), 5 glutathione, 0·2 cAMP, 1 fluo-3, pH 7·2 with CsOH. Cells were loaded with a high concentration (1 mM) of the fluorescent Ca^{2+} indicator fluo-3 in order to visualize Ca^{2+} sparks and to buffer cytoplasmic Ca^{2+}. Glutathione was included as an antioxidant to reduce phototoxicity. Na^+ was omitted from the patch pipette solution so that Na^+–Ca^{2+} exchange would be inhibited when extracellular Na^+ was replaced with Cs^+. During experiments, all bath solutions contained 10 μM TTX in order to block Na^+ currents. A constant holding potential of −75 mV was maintained throughout the experiments using an Axopatch 200A patch clamp amplifier (Axon Instruments, Foster City, CA, USA) and a Digidata 1200 (Axon Instruments) data acquisition system controlled by pCLAMP 6 software (Axon Instruments). The pCLAMP software was also used to control the timing of laser shutter opening, as well as solution exchanges (see below).

Laser scanning confocal fluorescence imaging

Cells were loaded with the Ca^{2+} indicator fluo-3 via the patch pipette (see above) and then imaged using a Noran Odyssey XL rapid 2-D laser scanning confocal microscopy system (Noran Instruments, Middleton, WI, USA) attached to a Zeiss Axiovert TV100 inverted microscope fitted with a ×40 water-immersion objective lens (Zeiss C-Apochromat 40/1.2 W Corr). The excitation wavelength of the argon–krypton laser was set to 488 nm, and fluorescence emission wavelengths greater than 510 nm were detected by the photomultiplier of the confocal system. Eighty sequential images were collected at 240 Hz (4 ms per frame). The size of each 2-D frame was 232 pixels × 98 pixels and the pixel size was 0·19 μm × 0·19 μm. To reduce photobleaching of the indicator

as well as phototoxicity to the cells, the laser was shuttered electronically and triggered to open by the patch clamp computer only during the 320 ms acquisition period. Fluorescence signals (F) were normalized by dividing them by the average fluorescence intensity at rest (F_0). This procedure removes the contribution of non-uniformities in dye concentration within the confocal plane and gives a signal that can be directly related to intracellular Ca^{2+} concentration (Cheng et al. 1995).

Image analysis

We used a computer-assisted method of identifying and measuring the characteristics of Ca^{2+} sparks on unfiltered images. In order to be considered a potential 'spark', increases in local fluorescence intensity had to meet the following three criteria: (1) the rate of increase in fluo-3 fluorescence over two successive frames had to be greater than twice the standard deviation of the background noise ($dF/dt_{potential\ spark} > 2\ \text{s.d.}\ dF/dt_{background\ noise}$); (2) for areas meeting the first criterion, fluorescence amplitude (F) could not fall more than 30% in the subsequent frame to remain a candidate; (3) areas satisfying the first two criteria had to also contain at least four contiguous 3 pixel × 3 pixel arrays (overlapping arrays permitted) meeting the first two criteria to remain a candidate. For selected sparks, intensity vs. time was measured from the average of the nine centremost pixels of the spark (a 3 pixel × 3 pixel array). Spark size was expressed in terms of full width at half-maximum intensity (FWHM). Pixels contiguous to the centre of a selected spark, and whose intensity exceeded half of the maximum intensity, were included in this area. These regions were usually smaller than what appeared by eye to be the outer dimension of the spark.

Image presentation

Spark frequency and location can be appreciated more readily in still pictures by preparing a 3-D image stack of 2-D image frames in temporal sequence, beginning with time 0 at the top and progressing to 320 ms at the bottom. Low intensity pixels are rendered semi-translucent and the stack of frames is viewed on end from the top so that all of the frames are superimposed upon each other. In this fashion, all the sparks occurring during the acquisition period can be displayed at once in a 2-D representation. A pseudo-linescan image ('X vs. time') can also be constructed from the 3-D image stack by sectioning through the stack at any horizontal line. This facilitates comparison with other investigators who record Ca^{2+} sparks directly as linescans.

Solution exchange

Bath solution was exchanged using a rapid solution switcher described previously (Goldhaber et al. 1991). The device exchanges the bath solution surrounding the myocyte by 90% within 200 ms. Solution switches were controlled by the pCLAMP software.

RESULTS

Characteristics of sparks under control conditions

We first characterized Ca^{2+} sparks under our control experimental conditions using high-speed 2-D confocal microscopy. Figure 1 shows a series of 2-D images at 4 ms intervals that illustrate the onset and decay of a single spontaneous Ca^{2+} spark. Under resting conditions, with normal external [Na^+] and at physiological holding potential (−75 mV), sparks were observed infrequently (1·0 ± 0·2 sparks (100 μm^2 s)$^{-1}$; mean ± s.e.m.) during a 320 ms acquisition period, suggesting a low activity of SR Ca^{2+}-

release channels under these conditions. A total of 91 sparks in 13 cells from 11 animals were analysed. Sparks varied in intensity (mean $F/F_0 = 2\cdot63 \pm 0\cdot11$), size (mean area at FWHM = $3\cdot4 \pm 0\cdot2\ \mu m^2$), and half-time (mean half-time measured at the 3 pixel × 3 pixel array at the spark centre = $8\cdot4 \pm 0\cdot5$ ms), as well as location (Fig. 2A and C). A stack presentation of a myocyte is illustrated in Fig. 2A. Note that three spontaneous sparks occurred during the 320 ms acquisition period. The three sparks were clearly visible in the 2-D stack whereas only two of the three could be seen in the corresponding pseudo-linescan (Fig. 2B). These data illustrate the dependence of spark detection on linescan position.

Characteristics of sparks following removal of extracellular sodium

To determine the effect of Na^+ withdrawal on spark behaviour, extracellular Na^+ was removed by substituting Cs^+ for Na^+ in the bath solution using the rapid solution switcher. The switch was timed so that the solution bathing the cell was completely exchanged 200 ms before acquisition of images began. Perfusion with Na^+-free solution continued throughout the duration of image acquisition (another 320 ms, total = 520 ms). Na^+-containing control solution was then returned to the bath. Since the cell was dialysed for at least 5 min with a pipette solution containing no Na^+, removal of extracellular Na^+ is expected to halt or transiently reverse Na^+–Ca^{2+} exchange. Figure 2C shows the effects of extracellular Na^+ removal on the same cell

illustrated in Fig. 2A. Note that there were now six sparks visible during the 320 ms acquisition period in Fig. 2C, although the corresponding pseudo-linescan shown in Fig. 2D revealed only two of the six sparks. Overall, we found an approximately fourfold increase in spark frequency (from $1\cdot0 \pm 0\cdot2$ to $4\cdot2 \pm 0\cdot8$ sparks $(100\ \mu m^2\ s)^{-1}$; $P < 0\cdot001$, Student's paired t test for 14 interventions in 5 cells) during this brief period of Na^+-free perfusion (Fig. 3). When Na^+ was reapplied the spark frequency returned to baseline (not shown). Na^+ could be repeatedly removed and reapplied with similar results.

We also assessed whether Na^+-free perfusion altered the intensity, size or time course of the Ca^{2+} spark. We analysed a total of 91 sparks under control conditions and 151 sparks during perfusion with Na^+-free solution. Na^+-free perfusion had no significant influence on the size (FWHM) of the sparks ($3\cdot4 \pm 0\cdot2\ \mu m^2$ under control conditions and $3\cdot7 \pm 0\cdot2\ \mu m^2$ during Na^+-free perfusion, $P = 0\cdot38$) or their intensity (F/F_0: control, $2\cdot63 \pm 0\cdot11$; Na^+ free, $2\cdot45 \pm 0\cdot07$; $P = 0\cdot17$; Fig. 4). The half-time for the declining phase of the centremost portion of the Ca^{2+} spark (a 3 pixel × 3 pixel array) was also unaffected by Na^+ removal ($8\cdot4 \pm 0\cdot5$ ms under control conditions, and $8\cdot5 \pm 0\cdot3$ ms during Na^+-free perfusion, $P = 0\cdot82$; Fig. 5). Likewise, there was no significant difference in the time constant for the declining phase when we considered the spread of the entire spark over an area within a $3\ \mu m$ radius of the spark centre ($31\cdot7 \pm 1\cdot64$ ms under control conditions *vs.* $31\cdot0 \pm 1\cdot9$ ms
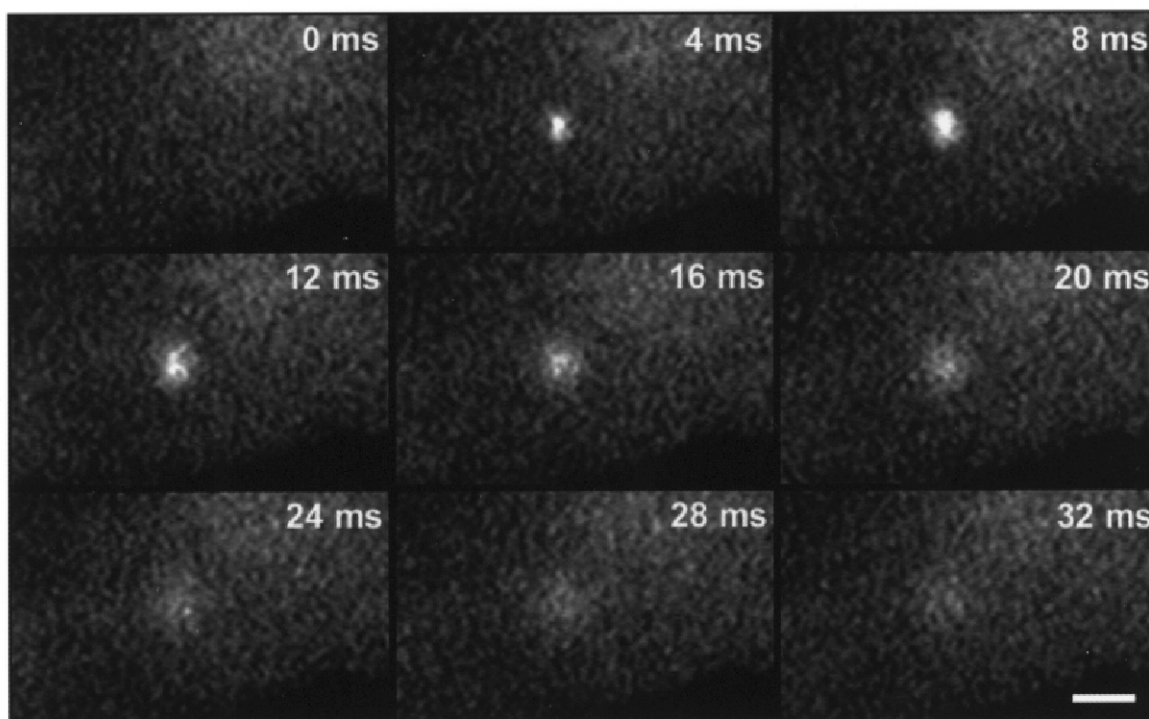

Figure 1. High speed 2-D confocal images of a spontaneous Ca^{2+} spark in an adult rat ventricular myocyte loaded with fluo-3 via the patch pipette

The frame rate is 240 Hz (4 ms per frame) and the holding potential is −75 mV. These images were filtered using a 3 × 3 low-pass smoothing algorithm. Scale bar, $5\ \mu m$.
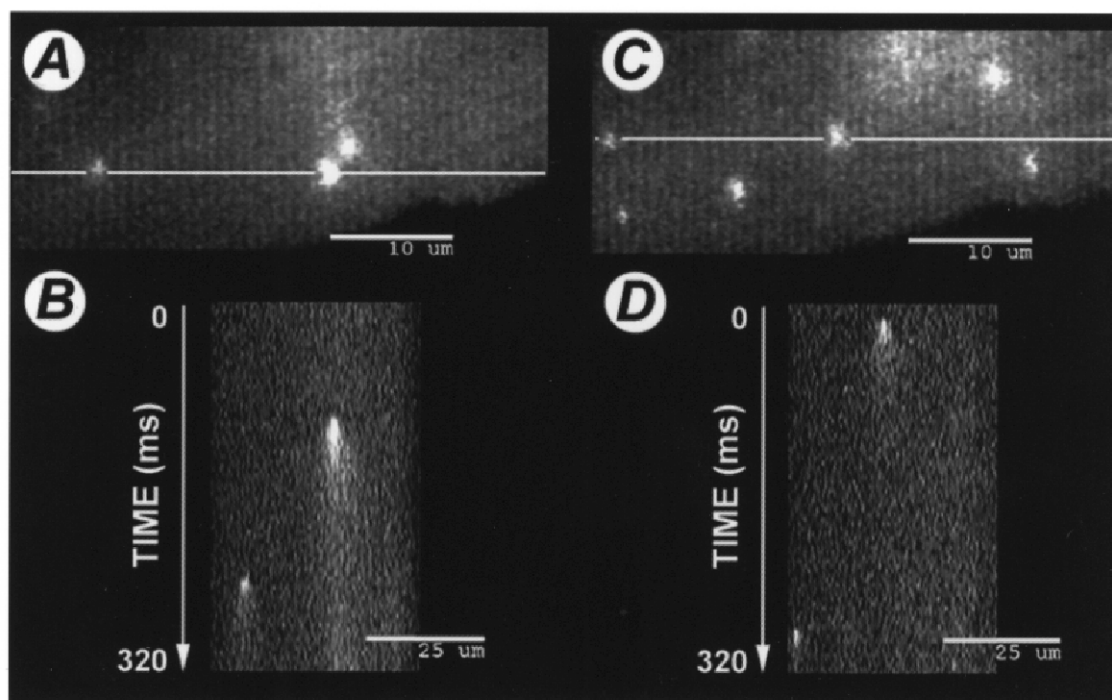
Figure 2. Effect of extracellular Na⁺ removal on Ca²⁺ sparks

A, stacked image (see Methods for details) of spontaneously occurring Ca^{2+} sparks during a 320 ms acquisition period in a patch clamped ventricular myocyte loaded with 1 mM fluo-3 via the patch pipette under control conditions, with normal extracellular [Na⁺]. Note that there are three sparks visible. The white line intersecting two of the sparks indicates where the stack was 'sectioned' to produce the corresponding pseudo-linescan image shown below in *B* ('*X vs.* time'). Note that only two of the three sparks revealed in the 2-D stack are found by the linescan. *C*, stacked image of the same cell, obtained during a 320 ms acquistion period beginning 200 ms after removal of extracellular Na⁺. Note that there are now six sparks visible on the 2-D stack during this brief exposure to Na⁺-free solution, whereas only two sparks are visible in *D*, the corresponding linescan.

during Na⁺-free perfusion, $P = 0.79$). Thus, brief extracellular Na⁺ removal significantly increased the frequency of spontaneous Ca²⁺ sparks without detectably altering their intensity, size or kinetics.

Effect of Na⁺ removal on intracellular Ca²⁺

To determine whether the increase in spark frequency could be explained by an increase in resting bulk cytoplasmic Ca²⁺

concentration during extracellular Na⁺ removal, we measured background fluorescence before and after extracellular Na⁺ removal. During Na⁺-free perfusion, we found no significant increase in resting fluorescence locally at the sites of the subsequent Ca²⁺ sparks (pixel intensity 50 ± 3.4 with Na⁺ present *vs.* 52 ± 2.2 following removal of extracellular Na⁺, $P = 0.52$). Likewise, the resting fluorescence averaged over the entire frame was not significantly increased by Na⁺
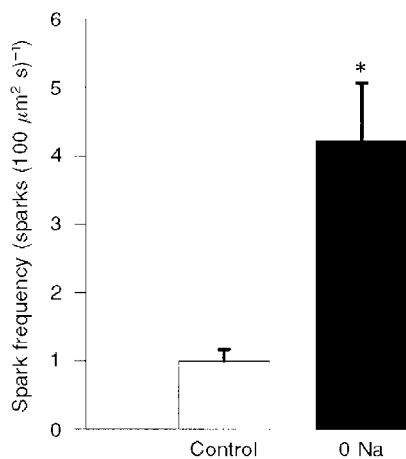

Figure 3. Spark frequency (in sparks (100 μm² s)⁻¹) under control conditions and during Na⁺-free (0 Na) perfusion

Results are means ± S.E.M. There was a fourfold increase in spark frequency during perfusion with Na⁺-free solution. *$P < 0.001$, Student's paired t test.
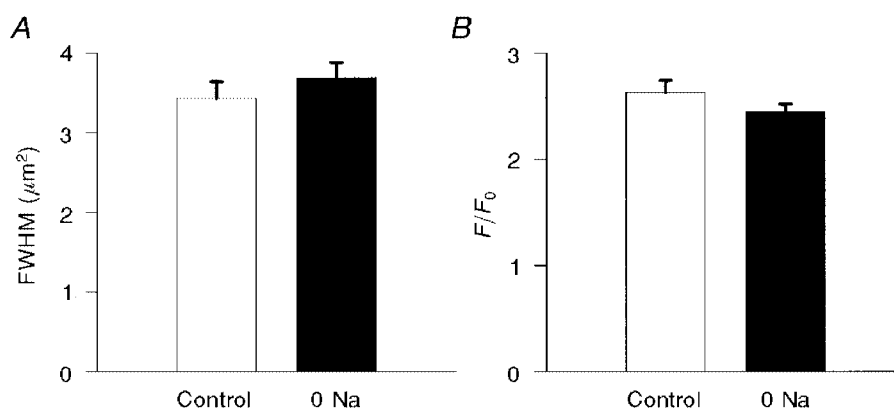
Figure 4. Spark area (in μm^2 using the FWHM criteria; *A*) and peak intensity (F/F_0; *B*) under control conditions and during Na^+-free (0 Na) perfusion

Results are means ± S.E.M. Removal of extracellular Na^+ had no significant effect on either parameter.

removal (data not shown). Thus, Na^+ removal for this brief period did not increase the global cytoplasmic $[Ca^{2+}]$ to a level sufficient to account for the increase in spark frequency that we observed.

Effect of Na^+ removal on SR Ca^{2+} content

SR Ca^{2+} content may elevate spark frequency (Lukyanenko *et al.* 1996; Satoh *et al.* 1997), although this is controversial (Song *et al.* 1997). To determine whether SR Ca^{2+} content had increased during Na^+-free perfusion, we measured SR Ca^{2+} content in our preparation before and during removal of external Na^+ by applying caffeine (5 mM) to the bath solution surrounding the cell for 750 ms. The observed caffeine-induced increase in cytoplasmic Ca^{2+} fluorescence was recorded at a frame rate of 30 Hz. Na^+ removal had no effect on SR Ca^{2+} release (control $\Delta F = 122 \pm 8.7$ *vs.* Na^+-free $\Delta F = 121 \pm 10.4$ arbitrary units, $P = 0.81$, Student's paired *t* test in 9 cells from 3 animals; Fig. 6). These results indicate that SR Ca^{2+} content remained stable during our experimental protocol. Even when 10 mM Na^+ was included in the pipette solution to *facilitate* reverse Na^+–Ca^{2+} exchange, there was still no significant increase in SR Ca^{2+} release during Na^+-free perfusion (data not shown).

DISCUSSION

Our findings indicate that brief removal of extracellular Na^+ leads to an increase in Ca^{2+} spark production, without altering the individual characteristics of the Ca^{2+} spark. These changes in spark frequency are not due to increases in either bulk cytoplasmic Ca^{2+} concentration or SR Ca^{2+} content, and thus strongly support the microdomain hypothesis.

There are three possible explanations for our findings. The first possibility is that Na^+ withdrawal leads to transient reverse Na^+–Ca^{2+} exchange, causing Ca^{2+} entry into a restricted space that is not well buffered by fluo-3. This in turn produces sparks by directly activating RyRs. A second possibility is that reverse exchange does not directly activate sparks, but increases $[Ca^{2+}]$ in the vicinity of the

RyRs so that there is a greater probability that a subsequent spontaneous L-type Ca^{2+} channel opening will produce a spark. The third possibility is that with forward exchange inhibited, either SR Ca^{2+} leak or a combination of Ca^{2+} leak and spontaneous L-type Ca^{2+} channel opening increases the local $[Ca^{2+}]$ in the vicinity of the RyRs, thereby increasing the probability of spark production. Since we have done
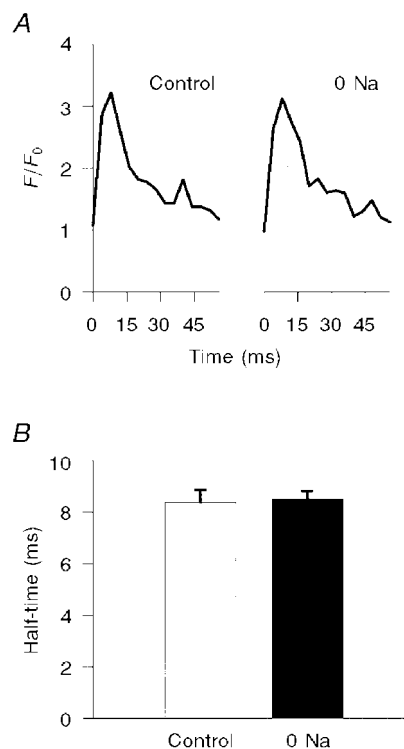

Figure 5. Time constant for the declining phase of the Ca^{2+} spark (in ms) under control conditions, and during perfusion with Na^+-free solution

A, representative traces of spark intensity *vs.* time when measuring only the nine centremost pixels of the spark. The control trace is shown on the left; the trace on the right (0 Na) was obtained during Na^+-free perfusion. *B*, corresponding plots of summary data (means ± S.E.M.).

nothing to change the probability of Ca^{2+} channel opening, the last two explanations are more or less equivalent.

We believe the third possibility to be the most likely for two reasons. First, the results of López-López *et al.* (1995) would argue against direct activation of RyRs by reverse exchange. Second, we tried to limit reverse $Na^+–Ca^{2+}$ exchange by excluding Na^+ from the pipette solution and dialysing the cell for at least 5–10 min before removing external Na^+. However, at the present time we are unable to measure cleft space Ca^{2+} directly. Thus, we cannot absolutely exclude the possibility that residual Na^+ in the cell cytoplasm allowed Ca^{2+} entry into the cleft via reverse $Na^+–Ca^{2+}$ exchange. We are confident that there was no significant increase in bulk cytoplasmic $[Ca^{2+}]$ due to reverse $Na^+–Ca^{2+}$ exchange, since our system can reliably detect a 15 nM change in cytoplasmic Ca^{2+}. Furthermore, 1 mM fluo-3 in the pipette provided

additional cytoplasmic Ca^{2+} buffering, making it unlikely that a rise in cytoplasmic $[Ca^{2+}]$ was responsible for the increase in spark activity. If reverse $Na^+–Ca^{2+}$ exchange was indeed present, then the ability of $Na^+–Ca^{2+}$ exchange to modulate spark frequency in the face of this increased buffering suggests that the effect of the exchanger is fairly robust. We also saw no increase in SR Ca^{2+} content that might suggest an increase in spark frequency due to SR Ca^{2+} loading via reverse $Na^+–Ca^{2+}$ exchange.

López-López *et al.* (1995) have shown that reverse $Na^+–Ca^{2+}$ exchange cannot trigger Ca^{2+} sparks directly. Their study specifically tested the ability of reverse $Na^+–Ca^{2+}$ exchange to trigger Ca^{2+} sparks in the absence of Ca^{2+} entry through L-type Ca^{2+} channels (by depolarizing to membrane potentials high enough to produce Ca^{2+} entry via reverse $Na^+–Ca^{2+}$ exchange, while at the same time eliminating
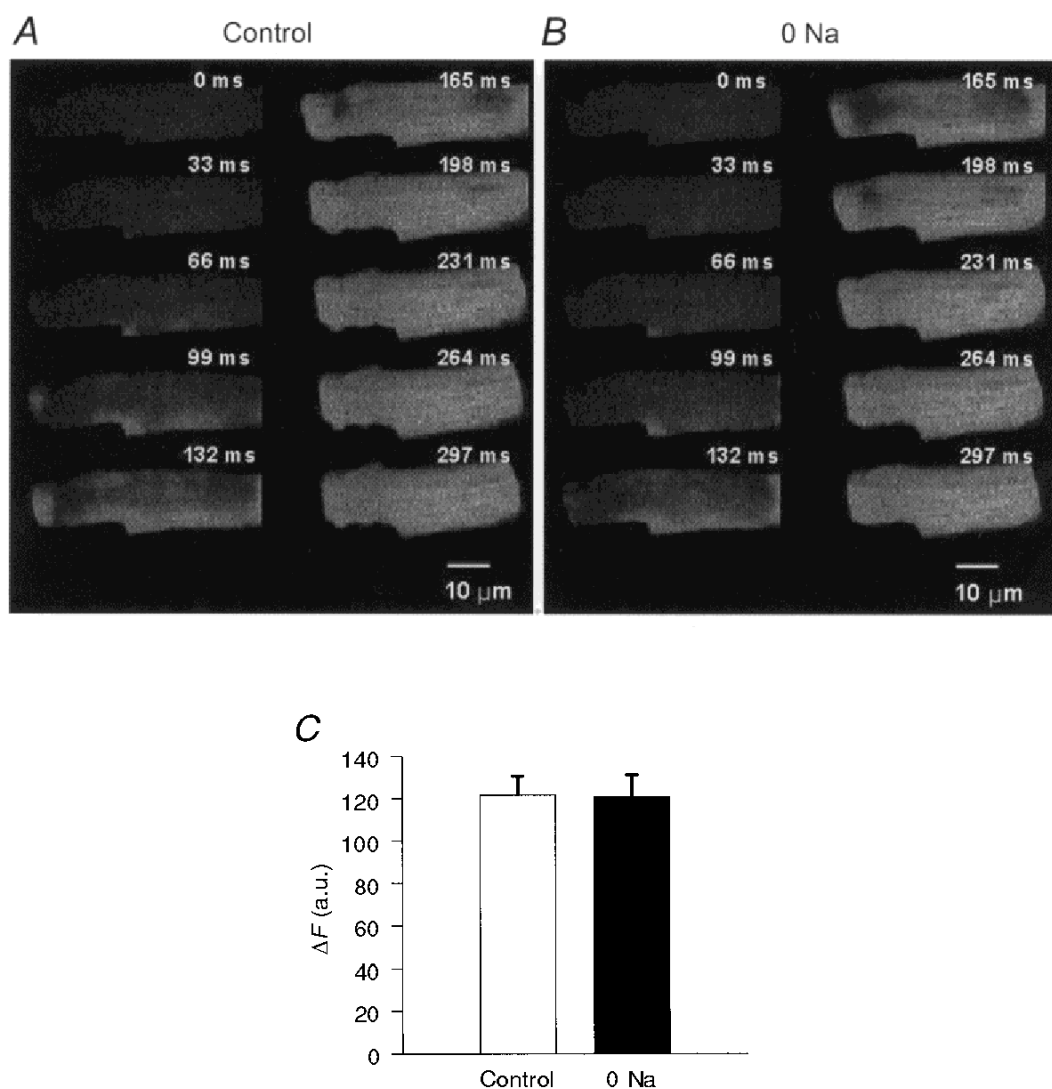

Figure 6. Effect of extracellular Na^+ removal on SR Ca^{2+} stores

Sequential images of a patch clamped rat ventricular myocyte loaded with fluo-3 obtained at a frame rate of 30 Hz (33 ms per frame) during a 750 ms application of 5 mM caffeine under control conditions (*A*) or following removal of bath Na^+ (0 Na) (*B*). *C*, summary data (means ± S.E.M.; $n = 9$ cells) of the fluorescence change (ΔF), in arbitrary units (a.u.) of pixel intensity, in response to 5 mM caffeine under control conditions and after removal of bath Na^+.

additional Ca^{2+} entry through L-type Ca^{2+} channels). Our experimental protocols were designed to modulate $Na^+–Ca^{2+}$ exchange activity *without* altering L-type Ca^{2+} channel activity. Membrane voltage was maintained at the resting potential, the extracellular Ca^{2+} concentration was constant, and we did not apply any agents known to influence Ca^{2+} channels. Thus our conditions were optimized to demonstrate how $Na^+–Ca^{2+}$ exchange might *modulate* the effectiveness of Ca^{2+} channels to induce sparks, i.e. how $Na^+–Ca^{2+}$ exchange might alter the gain of E–C coupling. A similar argument may explain why Gomez *et al.* (1996) failed to detect a change in spark frequency during inhibition of $Na^+–Ca^{2+}$ exchange using Na^+- and Ca^{2+}-free bath solutions. Removal of extracellular Ca^{2+} would have reduced single channel Ca^{2+} currents, and therefore the amount of Ca^{2+} entering the cleft when a Ca^{2+} channel opened. This would reduce the probability of triggering a spark when L-type Ca^{2+} channels open, and counteract any increase in spark probability resulting from a rise in cleft space $[Ca^{2+}]$ due to inhibition of $Na^+–Ca^{2+}$ exchange. Another potential drawback of these previous studies was that they used linescan mode rather than rapid 2-D acquisition. As illustrated in Fig. 2, the linescan mode may not be optimally suited for examining changes in spark frequency because of the limited spatial sampling. Our method, using rapid 2-D confocal scanning, enables us to sample an area approximately 100 times larger at high temporal resolution.

Our findings suggest that in a system where SR Ca^{2+} load and Ca^{2+} entry through L-type Ca^{2+} channels are unaltered, $Na^+–Ca^{2+}$ exchange has a significant influence on the frequency of Ca^{2+} sparks, presumably by setting the Ca^{2+} concentration in the local vicinity of the RyRs. This influences how much additional Ca^{2+} is required to reach the threshold for a local all-or-none Ca^{2+}-release event (Lipp & Niggli, 1994). Our results imply that at diastolic membrane potentials, forward $Na^+–Ca^{2+}$ exchange functions to keep the $[Ca^{2+}]$ low in the cleft by removing Ca^{2+} that leaks out of the SR or that enters during stochastic openings of Ca^{2+} channels. In the absence of $Na^+–Ca^{2+}$ exchange, Ca^{2+} accumulates in the cleft and it takes less additional Ca^{2+} entry through L-type Ca^{2+} channels to activate RyRs. This is direct experimental evidence supporting the recent argument by Litwin *et al.* (1998) to explain how $Na^+–Ca^{2+}$ exchange might regulate the gain of Ca^{2+}-induced Ca^{2+} release in cardiac muscle. They speculate that a local increase in $[Ca^{2+}]$ in the region of the RyR produces a shift along the flat foot of the sigmoidal curve relating Ca^{2+} concentration to the open probability of the RyR. By raising baseline $[Ca^{2+}]$ close to that at the steep part of the curve, less additional Ca^{2+} is required (added by the opening of an L-type Ca^{2+} channel, for example) to trigger RyR opening, in essence, a non-linear summation of triggers.

We conclude that the basal activity of $Na^+–Ca^{2+}$ exchange is an important factor regulating Ca^{2+} concentration in the diadic cleft, which has important consequences for spark activity and E–C coupling gain.

Adachi-Akahane, S., Cleemann, L. & Morad, M. (1996). Cross-signaling between L-type Ca^{2+} channels and ryanodine receptors in rat ventricular myocytes. *Journal of General Physiology* **108**, 435–454.

Cheng, H., Cannell, M. B. & Lederer, W. J. (1995). Partial inhibition of Ca^{2+} current by methoxyverapamil (D600) reveals spatial nonuniformities in $[Ca^{2+}]_i$ during excitation-contraction coupling in cardiac myocytes. *Circulation Research* **76**, 236–241.

Cheng, H., Lederer, W. J. & Cannell, M. B. (1993). Calcium sparks – elementary events underlying excitation-contraction coupling in heart muscle. *Science* **262**, 740–744.

Cleemann, L., Wang, W. & Morad, M. (1998). Two-dimensional confocal images of organization, density, and gating of focal Ca^{2+} release sites in rat cardiac myocytes. *Proceedings of the National Academy of Sciences of the USA* **95**, 10984–10989.

Copello, J. A., Barg, S., Onoue, H. & Fleischer, S. (1997). Heterogeneity of Ca^{2+} gating of skeletal muscle and cardiac ryanodine receptors. *Biophysical Journal* **73**, 141–156.

Frank, J. S., Mottino, G., Reid, D., Molday, R. S. & Philipson, K. D. (1992). Distribution of the Na^+-Ca^{2+} exchange protein in mammalian cardiac myocytes: an immunofluorescence and immunocolloidal gold-labeling study. *Journal of Cell Biology* **117**, 337–345.

Goldhaber, J. I., Parker, J. M. & Weiss, J. N. (1991). Mechanisms of excitation–contraction coupling failure during metabolic inhibition in guinea-pig ventricular myocytes. *Journal of Physiology* **443**, 371–386.

Gomez, A. M., Cheng, H., Lederer, W. J. & Bers, D. M. (1996). Ca^{2+} diffusion and sarcoplasmic reticulum transport both contribute to $[Ca^{2+}]_i$ decline during Ca^{2+} sparks in rat ventricular myocytes. *Journal of Physiology* **496**, 575–581.

Györke, S. & Fill, M. (1993). Ryanodine receptor adaptation – control mechanism of Ca^{2+}-induced Ca^{2+} release in heart. *Science* **260**, 807–809.

LeBlanc, N. & Hume, J. R. (1990). Sodium current-induced release of calcium from cardiac sarcoplasmic reticulum. *Science* **248**, 372–376.

Levi, A. J., Spitzer, K. W., Kohmoto, O. & Bridge, J. H. B. (1994). Depolarization-induced Ca entry via Na-Ca exchange triggers SR release in guinea pig cardiac myocytes. *American Journal of Physiology* **266**, H1422–1433.

Lipp, P. & Niggli, E. (1994). Sodium current-induced calcium signals in isolated guinea-pig ventricular myocytes. *Journal of Physiology* **474**, 439–446.

Litwin, S. E., Li, J. & Bridge, J. H. (1998). Na-Ca exchange and the trigger for sarcoplasmic reticulum Ca release: studies in adult rabbit ventricular myocytes. *Biophysical Journal* **75**, 359–371.

López-López, J. R., Shacklock, P. S., Balke, C. W. & Wier, W. G. (1994). Local, stochastic release of Ca^{2+} in voltage-clamped rat heart cells: visualization with confocal microscopy. *Journal of Physiology* **480**, 21–29.

López-López, J. R., Shacklock, P. S., Balke, C. W. & Wier, W. G. (1995). Local calcium transients triggered by single L-type calcium channel currents in cardiac cells. *Science* **268**, 1042–1045.

Lukyanenko, V., Györke, I. & Györke, S. (1996). Regulation of calcium release by calcium inside the sarcoplasmic reticulum in ventricular myocytes. *Pflügers Archiv* **432**, 1047–1054.

Mitra, R. & Morad, M. (1985). A uniform enzymatic method for dissociation of myocytes from hearts and stomachs of vertebrates. *American Journal of Physiology* **249**, H1056–1060.

Satoh, H., Blatter, L. A. & Bers, D. M. (1997). Effects of $[Ca^{2+}]_i$, SR Ca^{2+} load, and rest on Ca^{2+} spark frequency in ventricular myocytes. *American Journal of Physiology* **272**, H657–668.

SHAM, J. S., CLEEMANN, L. & MORAD, M. (1992). Gating of the cardiac Ca^{2+} release channel: the role of Na^+ current and Na^+-Ca^{2+} exchange. *Science* **255**, 850–853.

SHAM, J. S., CLEEMANN, L. & MORAD, M. (1995). Functional coupling of Ca^{2+} channels and ryanodine receptors in cardiac myocytes. *Proceedings of the National Academy of Sciences of the USA* **92**, 121–125.

SIPIDO, K. R., MAES, M. & VAN DE WERF, F. (1997). Low efficiency of Ca^{2+} entry through the Na^+-Ca^{2+} exchanger as trigger for Ca^{2+} release from the sarcoplasmic reticulum. A comparison between L-type Ca^{2+} current and reverse-mode Na^+-Ca^{2+} exchange. *Circulation Research* **81**, 1034–1044.

SONG, L. S., STERN, M. D., LAKATTA, E. G. & CHENG, H. (1997). Partial depletion of sarcoplasmic reticulum calcium does not prevent calcium sparks in rat ventricular myocytes. *Journal of Physiology* **505**, 665–675.

WIER, W. G., EGAN, T. M., LÓPEZ-LÓPEZ, J. R. & BALKE, C. W. (1994). Local control of excitation–contraction coupling in rat heart cells. *Journal of Physiology* **474**, 463–471.

Acknowledgements

Corresponding author

J. I. Goldhaber: Division of Cardiology, UCLA School of Medicine, 47-123 CHS, Box 951679, 10833 LeConte Avenue, Los Angeles, CA 90095-1679, USA.

Email: jgoldhaber@mednet.ucla.edu